

Electronic supplementary information

Template-free preparation of anthracite-based nitrogen-doped porous carbons for high-performance supercapacitors and efficient electrocatalysts for oxygen reduction reaction

Jiawei Qi, Bolin Jin, Peiyao Bai, Wendu Zhang and Lang Xu*

MOE Key Laboratory of Coal Processing and Efficient Utilization, School of Chemical Engineering and Technology, China University of Mining and Technology, 1 Daxue Road, Xuzhou, Jiangsu, 221116, China

*Corresponding author. *E-mail address: lang.xu@cumt.edu.cn* (L. Xu)

Table S1 Surface and pore properties of the ANPC-1 and ANPC-2 materials. ^a

Material	S_{BET} ($\text{m}^2 \text{g}^{-1}$)	S_{micro} ($\text{m}^2 \text{g}^{-1}$)	V_{pore} ($\text{cm}^3 \text{g}^{-1}$)	V_{micro} ($\text{cm}^3 \text{g}^{-1}$)
ANPC-1-800-0	2768.28	2512.76	1.363	1.128
ANPC-1-800-0.25	2271.05	1930.03	1.065	0.866
ANPC-1-800-1	1251.03	1142.19	0.568	0.456
ANPC-1-700-0.25	1990.55	1885.32	0.867	0.765
ANPC-1-900-0.25	2740.14	1404.37	1.666	0.605
ANPC-2-900-4	1654.08	1434.94	0.823	0.631
ANPC-2-900-6	2729.92	2344.92	1.318	1.005
ANPC-2-900-8	1911.54	1665.73	0.953	0.736
ANPC-2-800-6	2204.50	2004.56	1.086	0.861
ANPC-2-1000-6	2541.56	2054.74	1.328	0.896

^a S_{BET} : BET specific surface area; S_{micro} : micropore surface area based on the t-plot method; V_{pore} : pore volume;

V_{micro} : micropore volume based on the t-plot method.

Table S2 A comparison of BET specific surface area (S_{BET}) and specific capacitance (C_s) values of porous carbonaceous materials made from different carbon sources. ^a

Carbon source	S_{BET} ($\text{m}^2 \text{g}^{-1}$)	C_s (F g^{-1})	Current density (A g^{-1})	Ref
Coal	902	230	1	S1
Coal	621.15	227	1	S2
Coal	1872	211	1	S3
Agarose	2666	214	0.2	S4
Wheat flour	995	178.5	0.5	S5
Corn straws	2790.4	327	0.2	S6
Anthracite	2271.05	346	0.5	This work

^a All the C_s values in the table were obtained from the three-electrode system using 6 M KOH as the electrolyte.

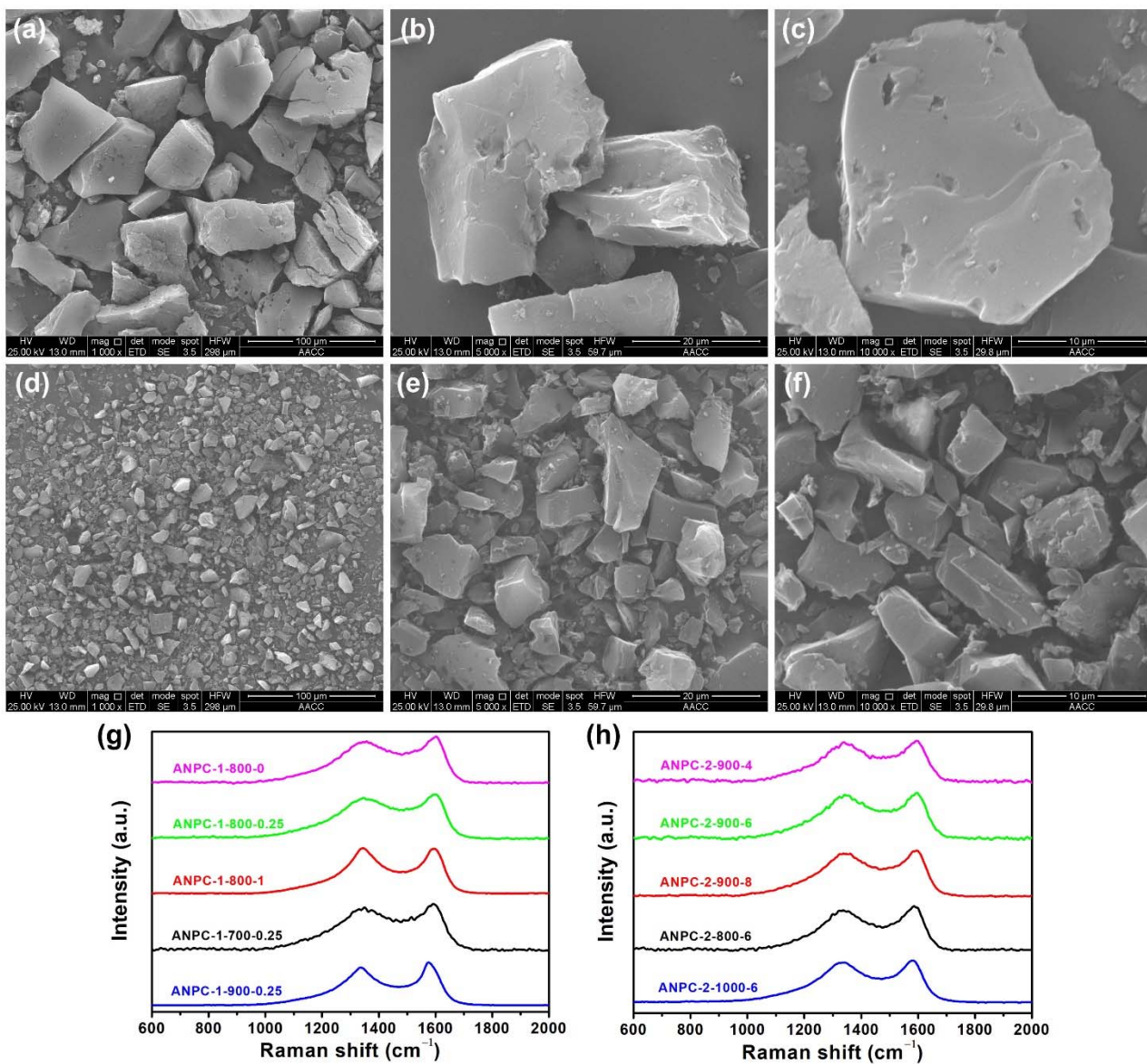


Fig. S1 SEM images of (a-c) ANPC-1-800-0.25 and (d-f) ANPC-2-900-6 with different magnifications (1k: a, d; 5k: b, e; 10k: c, f). Raman spectra of (g) the ANPC-1 materials and (h) the ANPC-2 materials.

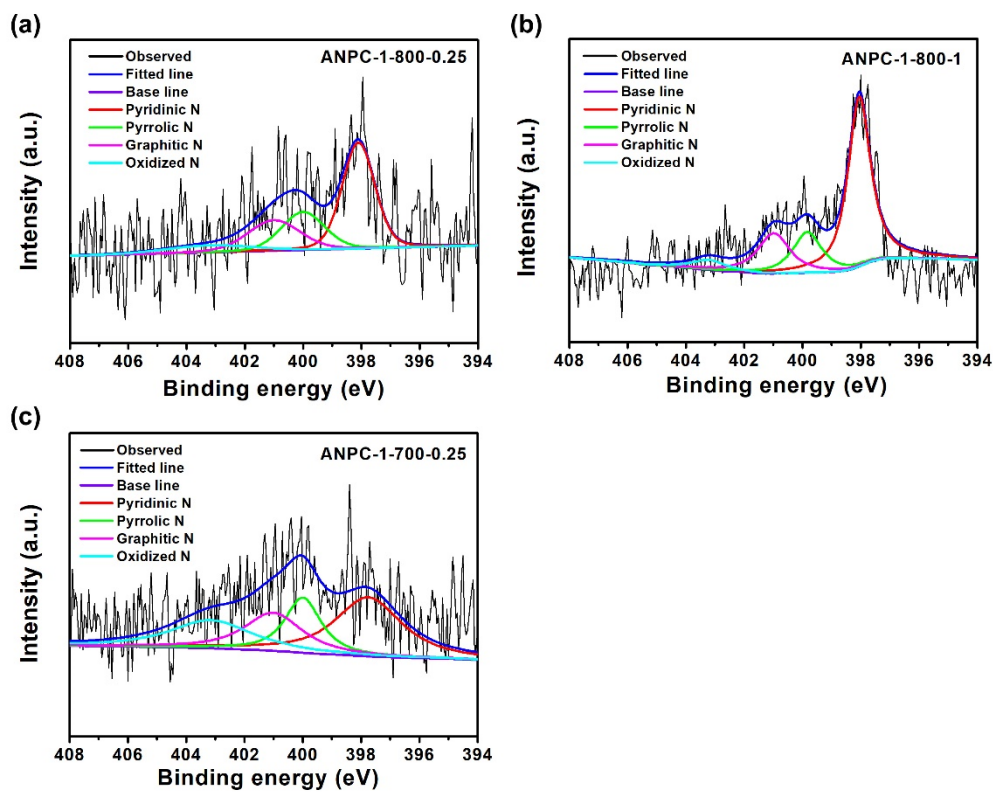


Fig. S2 High-resolution XPS N 1s spectra of (a) ANPC-1-800-0.25, (b) ANPC-1-800-1 and (c) ANPC-1-700-0.25.

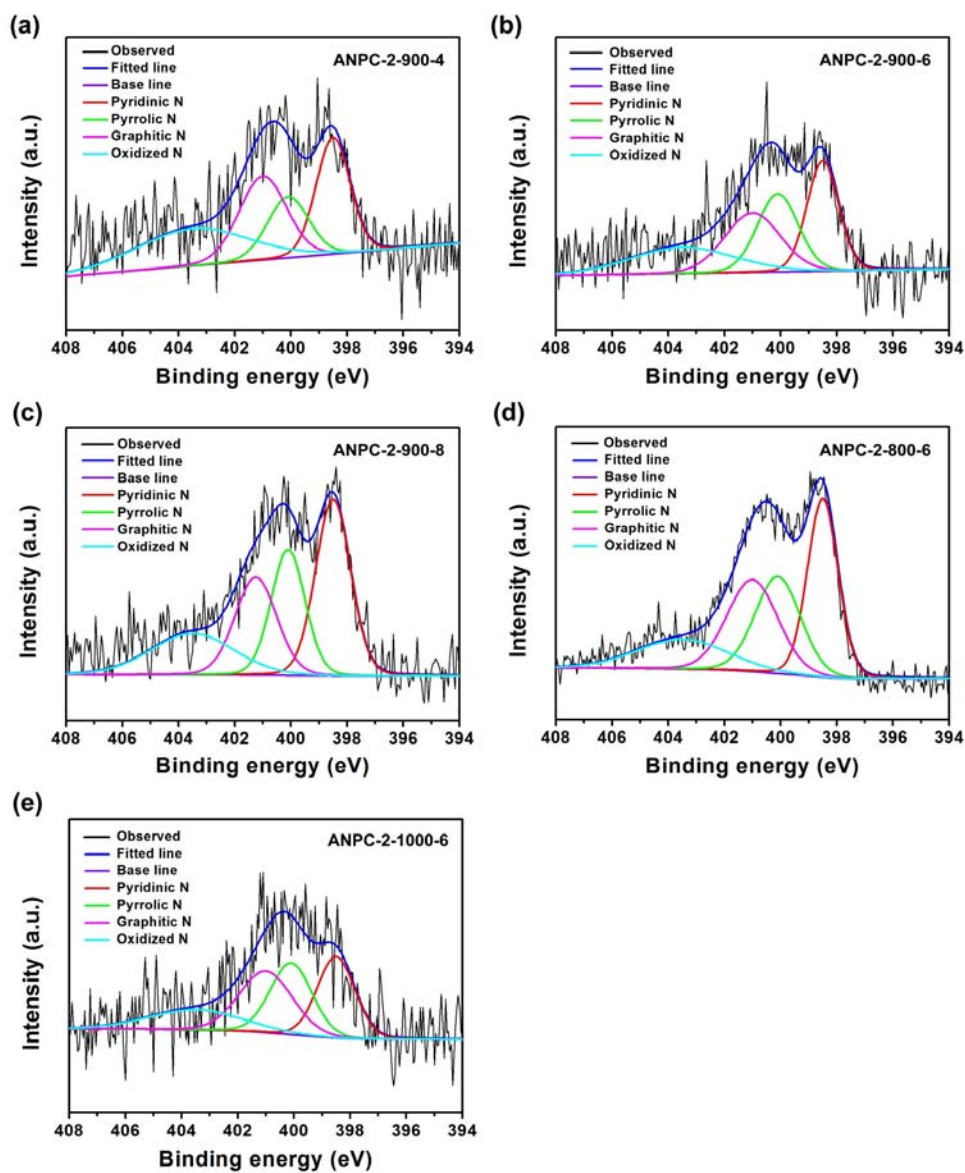


Fig. S3 High-resolution XPS N 1s spectra of (a) ANPC-2-900-4, (b) ANPC-2-900-6, (c) ANPC-2-900-8, (d) ANPC-2-800-6 and (e) ANPC-2-1000-6.

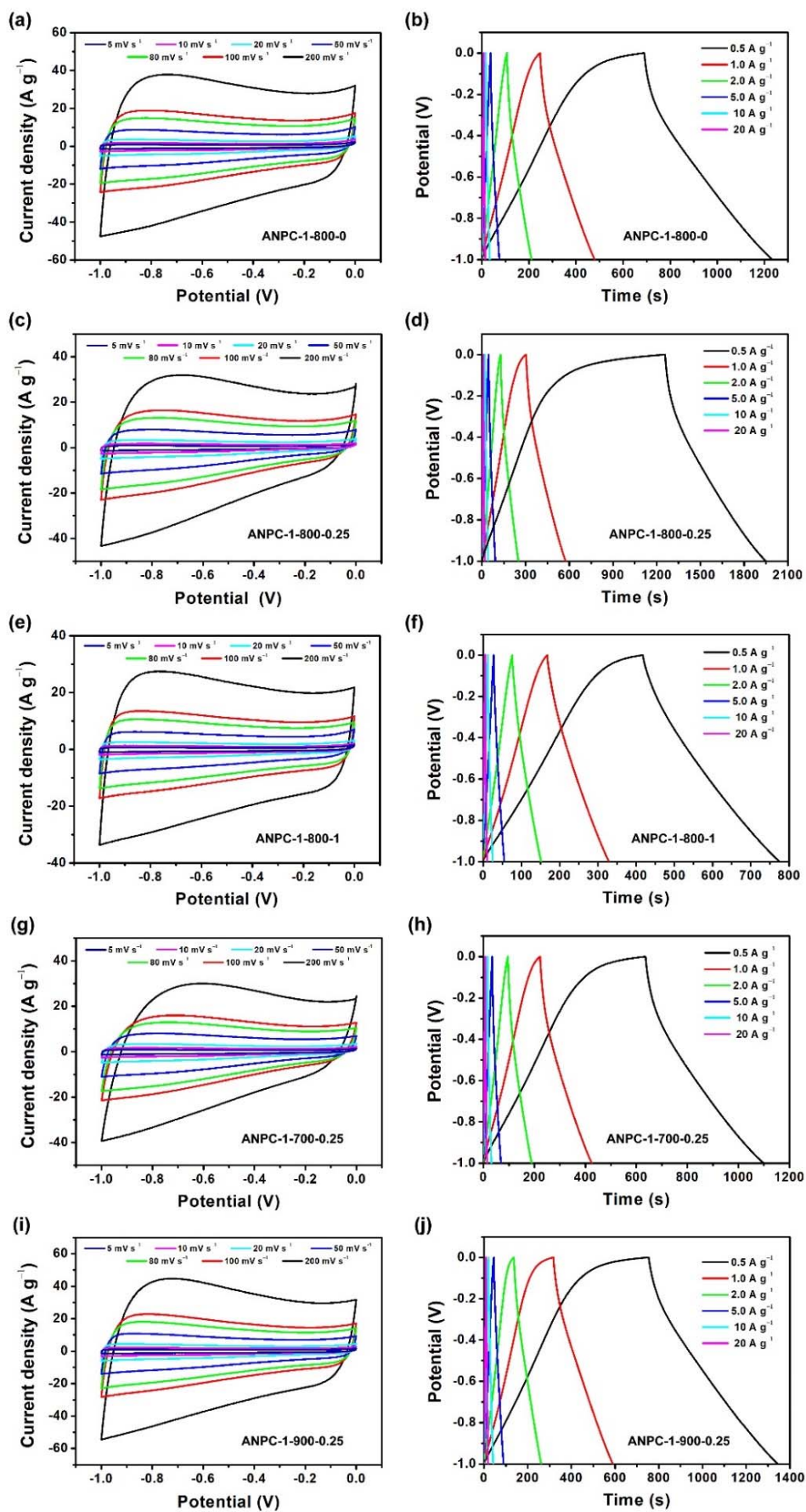


Fig. S4 CV curves of (a) ANPC-1-800-0, (c) ANPC-1-800-0.25, (e) ANPC-1-800-1, (g) ANPC-1-700-0.25 and (i) ANPC-1-900-0.25 at different scan rates; GCD curves of (b) ANPC-1-800-0, (d) ANPC-1-800-0.25, (f) ANPC-1-800-1, (h) ANPC-1-700-0.25 and (j) ANPC-1-900-0.25 at different charge/discharge current densities. All the measurements were taken in 6 M KOH.

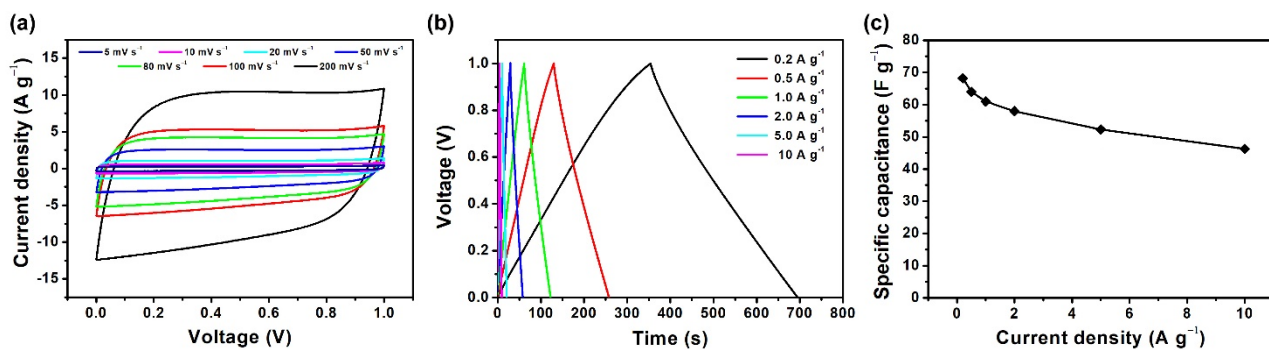


Fig. S5 (a) CV curves of the ANPC-1-800-0.25//ANPC-1-800-0.25 supercapacitor at different scan rates; (b) GCD curves of the ANPC-1-800-0.25//ANPC-1-800-0.25 supercapacitor at different charge/discharge current densities; (c) specific capacitances of the ANPC-1-800-0.25//ANPC-1-800-0.25 supercapacitor at different current densities. All the measurements were taken in 6 M KOH.

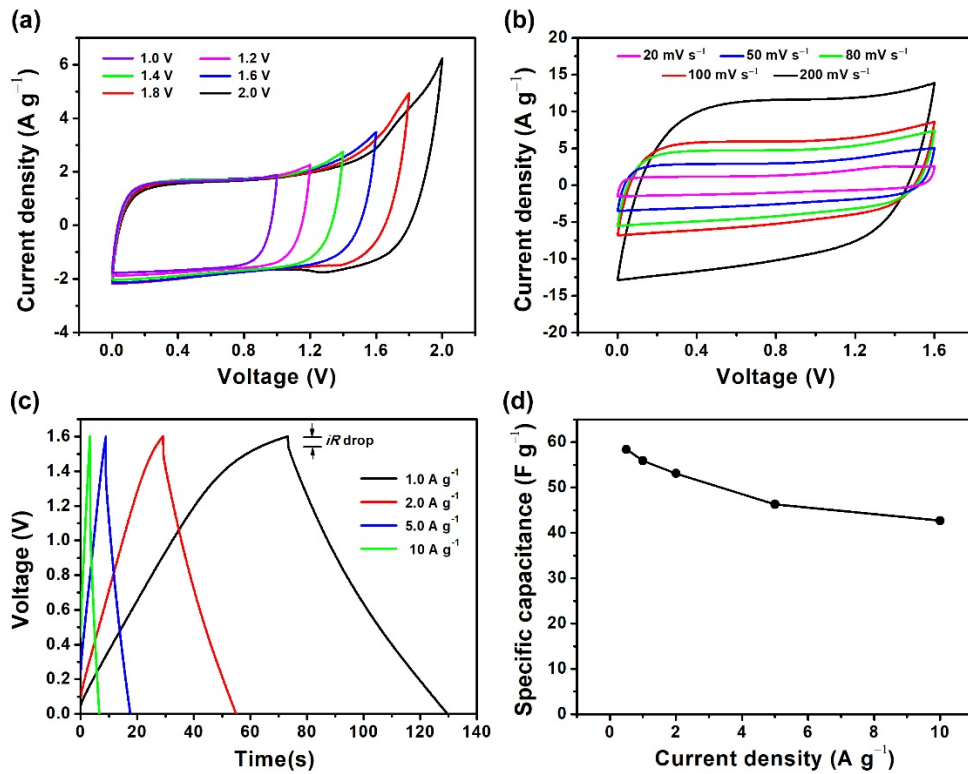


Fig. S6 (a) CV curves of the ANPC-1-800-0.25//ANPC-1-800-0.25 supercapacitor with different voltage windows at a scan rate of 50 mV s⁻¹; (b) CV curves of the ANPC-1-800-0.25//ANPC-1-800-0.25 supercapacitor at different scan rates; (c) GCD curves of the ANPC-1-800-0.25//ANPC-1-800-0.25 supercapacitor at different charge/discharge current densities; (d) specific capacitances of the ANPC-1-800-0.25//ANPC-1-800-0.25 supercapacitor at different current densities. All the measurements were taken in 1 M Na₂SO₄.

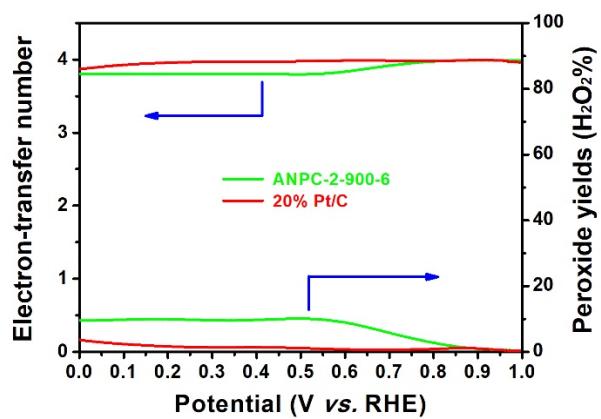


Fig. S7 RRDE measurements in 0.1 M KOH at 1600 rpm: the electron-transfer numbers and peroxide yield of ANPC-2-900-6 and 20% Pt/C across the potentials ranging from 0 to 1.0 V vs. RHE.

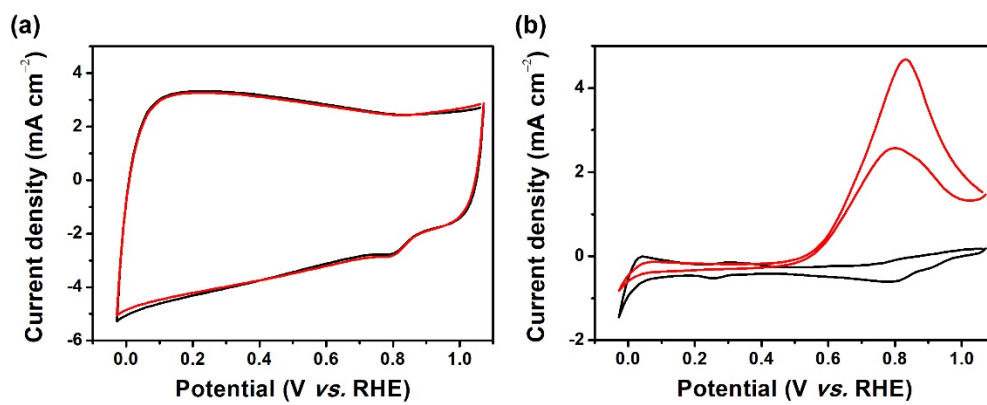


Fig. S8 CV curves of (a) ANPC-2-900-6 and (b) 20% Pt/C at the scan rate of 50 mV s⁻¹ in O₂ saturated 0.1 M KOH solution at 25 °C before (black) and after (red) the addition of 1 M methanol.

References

- S1. H. Zhao, L. Wang, D. Jia, W. Xia, J. Li and Z. Guo, *J. Mater. Chem. A*, 2014, **24**, 9338-9344.
- S2. M. Guo, J. Guo, F. Tong, D. Jia, W. Jia, J. Wu, L. Wang and Z. Sun, *RSC Adv.*, 2017, **7**, 45363-45368.
- S3. L. Wang, F. Sun, J. Gao, X. Pi, T. Pei, Z. Qie, G. Zhao and Y. Qin, *J. Taiwan Inst. Chem. Eng.*, 2018, **91**, 588-596.
- S4. B. You, F. Kang, P. Yin and Q. Zhang, *Carbon*, 2016, **103**, 9-15.
- S5. G. Lin, R. Ma, Y. Zhou, C. Hu, M. Yang, Q. Liu, S. Kaskel and J. Wang, *J. Colloid Interface Sci.*, 2018, **527**, 230-240.
- S6. Z. Qiu, Y. Wang, X. Bi, T. Zhou, J. Zhou, J. Zhao, Z. Miao, W. Yi, P. Fu and S. Zhuo, *J. Power Sources*, 2018, **376**, 82-90.